

ORIGINAL ARTICLE

Phenotypic heterogeneity in patients with *NEFL*-related Charcot–Marie–Tooth disease

Hye Jin Kim^{1,2}  | Sang Beom Kim³ | Hyun Su Kim⁴ | Hye Mi Kwon² | Jae Hong Park² | Ah Jin Lee⁵ | Si On Lim⁵ | Soo Hyun Nam⁶ | Young Bin Hong⁷ | Ki Wha Chung⁵  | Byung-Ok Choi^{1,2,6} 

¹Department of Health Sciences and Technology, SAIHST, Sungkyunkwan University, Seoul, Korea

²Department of Neurology, Samsung Medical Center, Sungkyunkwan University School of Medicine, Seoul, Korea

³Department of Neurology, Kyung Hee University Hospital at Gangdong, Kyung Hee University School of Medicine, Seoul, Republic of Korea

⁴Department of Radiology, Samsung Medical Center, Sungkyunkwan University School of Medicine, Seoul, Korea

⁵Department of Biological Sciences, Kongju National University, Gongju, Korea

⁶Stem Cell & Regenerative Medicine Institute, Samsung Medical Center, Seoul, Korea

⁷Department of Biochemistry, College of Medicine, Dong-A University, Busan, Korea

Correspondence

Byung-Ok Choi, Department of Neurology, Samsung Medical Center, Sungkyunkwan University School of Medicine, 81 Irwon-ro, Gangnam-gu, Seoul 06351, Korea.

Email: bochoi77@hanmail.net

Ki Wha Chung, Department of Biological Sciences, Kongju National University, 56 Gongjudaehak-ro, Gongju 32588, Korea.

Email: kwchung@kongju.ac.kr

Funding information

National Research Foundation, Grant/Award Number: 2019R1A2C1087547, 2020M3H4A1A03084600 and 2021R1A4A2001389; Korean Health Technology R&D Project, Ministry of Health and Welfare, Grant/Award Number: HI14C3484 and HI20C0039

Abstract

Charcot–Marie–Tooth disease (CMT) is the most common hereditary peripheral neuropathy. Mutations in the neurofilament light polypeptide (*NEFL*) gene produce diverse clinical phenotypes, including demyelinating (CMT1F), axonal (CMT2E), and intermediate (CMTDIG) neuropathies. From 2005 to 2020, 1,143 Korean CMT families underwent gene sequencing, and we investigated the clinical, genetic, and neuroimaging spectra of *NEFL*-related CMT patients. Ten *NEFL* mutations in 17 families (1.49%) were identified, of which three (p.L312P, p.Y443N, and p.K467N) were novel. Eight de novo cases were identified at a rate of 0.47 based on a cosegregation analysis. The age of onset was ≤ 3 years in five cases (13.5%). The patients revealed additional features including delayed walking, ataxia, dysphagia, dysarthria, dementia, ptosis, waddling gait, tremor, hearing loss, and abnormal visual evoked potential. Signs of ataxia were found in 26 patients (70.3%). In leg MRI analyses, various degrees of intramuscular fat infiltration were found. All compartments were evenly affected in CMT1F patients. The anterior and anterolateral compartments were affected in CMT2E, and the posterior compartment was affected in CMTDIG. Thus, *NEFL*-related CMT patients showed phenotypic heterogeneities. This study's clinical, genetic, and neuroimaging results could be helpful in the evaluation of novel *NEFL* variants and differential diagnosis against other CMT subtypes.

Hye Jin Kim and Sang Beom Kim contributed equally.

This is an open access article under the terms of the Creative Commons Attribution-NonCommercial-NoDerivs License, which permits use and distribution in any medium, provided the original work is properly cited, the use is non-commercial and no modifications or adaptations are made.

© 2022 The Authors. *Molecular Genetics & Genomic Medicine* published by Wiley Periodicals LLC.

KEYWORDSCharcot–Marie–Tooth disease, heterogeneity, *NEFL*, phenotype

1 | INTRODUCTION

Charcot–Marie–Tooth disease (CMT), also called hereditary motor and sensory neuropathy, is a group of genetically and clinically heterogeneous disorders. It is characterized by progressive, distal-predominant weakness, amyotrophy, and sensory loss (Rossor et al., 2013). CMT can be divided into demyelinating neuropathy CMT type 1 (CMT1) and axonal neuropathy CMT type 2 (CMT2), which have median motor nerve conduction velocities (MNCVs) below or above 38 m/s, respectively, and the intermediate CMT subtype, which has median MNCVs of 25–45 m/s (Saporta et al., 2011).

There is genetic overlap among the CMT subtypes, and mutation in the neurofilament light-chain polypeptide (*NEFL*) gene exhibits diverse phenotypic subtypes (Mersianova et al., 2000). A mutation in *NEFL* was first reported to cause autosomal dominant CMT type 2E (CMT2E), and then, several other mutations were subsequently revealed to be associated with autosomal dominant CMT type 1F (CMT1F), dominant intermediate CMT type G (CMTDIG), and autosomal recessive CMT (Abe et al., 2009; Berciano et al., 2015; Jordanova et al., 2003; Mersianova et al., 2000; Yum et al., 2009).

Neurofilaments are formed by the polymerization of three subunits, the neurofilament light, medium, and heavy polypeptides (Yuan et al., 2012). *NEFL* encodes a light polypeptide of three subunits of neurofilaments, which are major components of the neuronal cytoskeleton that provides structural support. Mutations in *NEFL* cause failure to assemble with wild-type proteins or self-assemble, thereby affecting the neurofilament network and axonal transport (Yuan et al., 2012). Mutations in *NEFL* also affect the maturation of regenerating myelinated axons. In addition, *NEFL* can interact with *MTMR2*, a cause of CMT4B1, in both Schwann cells and neurons (Previtali et al., 2003). Therefore, mutations in *NEFL* can cause diverse CMT phenotypes. However, phenotypic characteristics and obvious genotype–phenotype correlations have not yet been established in Korean patients with *NEFL*-related CMT.

In this study, we describe 37 Korean *NEFL*-related CMT patients, including six patients with novel mutations, elucidating the clinical, electrophysiological, and neuroimaging phenotypic heterogeneities in patients who have CMT1F, CMT2E, or CMTDIG.

2 | PATIENTS AND METHODS

2.1 | Patients

Gene sequencing was performed for a cohort of 1,889 CMT patients from 1,143 unrelated Korean families from April 2005 to March 2020. From that cohort, we excluded 344 families with a *PMP22* duplication and further analyzed the 699 remaining families using whole-exome sequencing (WES). In that examination, we identified 17 CMT families with 10 *NEFL* mutations. Written informed consent was obtained from all participants in accordance with a protocol approved by the Institutional Review Board of Sungkyunkwan University, Samsung Medical Center (2014-08-057-002), and Kongju National University (KNU-IRB-2018-62).

2.2 | Clinical assessments

Clinical information included assessments of muscle atrophy, deep tendon reflex, and motor and sensory impairments. Flexor and extensor muscle strength was assessed manually with the standard Medical Research Council (MRC) scale (Paternostro-Sluga et al., 2008). To determine the presence of physical disability, two scales were used: a functional disability scale (FDS) (Birouk et al., 1998) and the CMT neuropathy score version 2 (CMTNS v2) (Sadjadi et al., 2014). Disease severity was identified for each patient using a nine-point FDS: 0, normal; 1, normal but with cramps and fatigability; 2, inability to run; 3, walking difficulty but still possible unaided; 4, walking with a cane; 5, walking with crutches; 6, walking with a walker; 7, wheelchair bound; and 8, bedridden. Sensory impairments were assessed based on the level and severity of pain, temperature, vibration, and position, and pain and vibration sense were compared. The age of onset was determined as the age at which symptoms, that is, distal muscle weakness, foot deformity, or sensory change, first appeared in the patient.

2.3 | Electrophysiological examinations

Nerve conduction studies of the median, ulnar, peroneal, tibial, and sural nerves were conducted using standard methods with surface stimulation and recording electrodes.

The motor nerve conduction velocities (MNCVs) and compound muscle action potentials (CMAPs) of the median and ulnar nerves were determined by stimulating the elbow and wrist while recording the abductor pollicis brevis and adductor digiti quinti, respectively. The MNCVs and CMAPs of the peroneal and tibial nerves were determined by stimulating the knee and ankle while recording the extensor digitorum brevis and adductor hallucis, respectively. CMAP amplitudes were determined from baseline to the negative peak values. Sensory nerve conduction velocities (SNCVs) were recorded for the median, ulnar, and sural nerves. SNCVs of the median and ulnar nerves were obtained by orthodromic scoring through the wrist part of the fingers. Sensory nerve action potentials (SNAPs) were measured from positive peaks to negative peaks.

2.4 | Mutational analysis

Genomic DNA was extracted from whole blood samples from Korean CMT families using a QIAamp DNA Mini Kit (Qiagen). The 17p12 (*PMP22*) duplication and deletion were first determined by hexaplex microsatellite PCR and real-time PCR in all the family samples. Mutations in *NEFL* were screened using WES (Lee et al., 2020) and confirmed by Sanger sequencing. Exome sequencing was conducted using a SureSelect Human All Exon 50 M Kit (Agilent Technologies) and HiSeq2000 and HiSeq2500 Genome Analyzers (Illumina). The human reference genome UCSC assembly hg19 (<http://genome.ucsc.edu>) was used to map the sequences. From the WES data, functionally significant variants (missense, nonsense, exonic indel, and splicing site variants) were selected first, and then unreported or rare variants with minor allele frequencies of ≤ 0.01 were further chosen in dbSNP154 (<http://www.ncbi.nlm.nih.gov>), the 1000 Genomes project database (<http://www.1000genomes.org/>), the Exome Variant Server (<http://evs.gs.washington.edu/EVS/>), the Exome Aggregation Consortium (ExAC) Browser (<http://exac.broadinstitute.org/>), and the Korean Reference Genome Database (KRGDB, <http://coda.nih.go.kr/coda/KRGDB/>).

2.5 | In silico analysis and determination of pathogenic mutations

A SeqStudio genetic analyzer (Life Technologies-Thermo Fisher Scientific) was used for Sanger sequencing to confirm candidate mutations. Conservation analyses of the protein sequences were performed using MEGA6, ver. 6.0 (<http://www.megasoftware.net/>). I-TASSER was used to predict the 3D structure of the NEFL protein to evaluate

the putative conformational changes caused by the mutations (<https://zhanglab.ccmb.med.umich.edu/I-TASSER>). To predict mutation effect, in silico analyses were performed with the algorithms of PolyPhen-2 (<http://genetics.bwh.harvard.edu/pph2/>), MUpro (<http://www.ics.uci.edu/~baldig/mutation>), and Fathmm (<http://fathmm.biocompute.org.uk/inherited.html>). The pathogenicity was basically determined according to the American College of Medical Genetics and Genomics (ACMG) guideline (Richards et al, 2015).

2.6 | Lower extremity MRI

Lower extremity axial magnetic resonance imagings (MRIs) of the pelvic girdle, bilateral thighs, and lower legs were reviewed. MRIs were taken using either a 1.5-T or 3.0-T MRI system (Avanto or Skyra, Siemens Healthcare). Based on the 5-point semiquantitative scale described by Goutallier et al. (1994) axial T1-weighted MRI turbo spin echo images of the thigh and lower leg muscles were graded for fat infiltration. Three levels (proximal, mid, and distal) were evaluated bilaterally for the thigh muscles, and two levels (proximal and distal) of the lower leg muscles were evaluated.

Cross-sectional areas of bilateral sciatic nerves were measured at three levels: hamstring tendon origin (level 1), where the uppermost part of the semimembranosus tendon is visualized; lesser trochanter of the femur (level 2), where it is visualized most prominently; gluteus maximus tendon insertion (level 3).

2.7 | Statistical analysis

Data are expressed as the mean \pm standard deviation. The statistical significance of the data was assessed as a pairwise comparison using Student's *t* test. The significance criterion was set at $p < 0.05$.

3 | RESULTS

3.1 | Identification of *NEFL* mutations in Korean CMT patients

We enrolled 1,143 CMT families and excluded 344 families who had *PMP22* duplication. Pathogenic or likely pathogenic *NEFL* mutations were identified in 37 CMT patients from 17 families (Table 1). All mutations identified in this study, except for the novel mutations, have been previously reported to cause CMT (<http://www.hgmd.cf.ac.uk/ac/index.php>).

TABLE 1 NEFL mutations identified in 17 Korean CMT families

Index family	Domain	Nucleotide change ^a	Amino acid change	dbSNP154	1000G ^b	EVS ^c	ExAC ^d	KRGDB ^e	GERP ^f	In silico analysis ^g				References
										PP2	MUpro	Fathmm	Inheritance	
CMT1F														
FC549	Head	c.23C>T	p.P8L	rs61491953	—	—	—	—	5.59	0.998*	-0.853*	-1.62*	De novo	Jordanova et al. (2003)
FC99	Head	c.65C>G	p.P22R	rs267607538	—	—	—	—	5.27	0.993*	-0.664*	-1.70*	De novo	Shin et al. (2008)
FC361	Head	c.64C>A	p.P22T	rs28928910	—	—	—	—	5.27	0.951*	-0.905*	-1.54*	De novo	Yoshihara et al. (2002)
FC7	Coil2B	c.1186G>A	p.E396K	rs62636503	—	—	—	—	5.91	1.000*	-0.873*	-3.21*	De novo	Berciano et al. (2015)
FC467														
CMT2E														
FC804, FC838	Coil2B	c.935T>C	p.L312P	—	—	—	—	—	5.58	0.999*	-1.000*	-2.65*	De novo (FC838)	This study
FC221, FC1037	Coil2B	c.1150A>T	p.I384F	—	—	—	—	—	5.78	1.000*	-0.826*	-2.57*	De novo	Choi et al. (2012)
FC154, FC330, FC441, FC984	Coil2B	c.1186G>A	p.E396K	rs62636503	—	—	—	—	5.91	1.000*	-0.873*	-3.21*	De novo (FC441, FC984)	Berciano et al. (2015)
CMT2E														
FC21	Coil2B	c.998T>C	p.L333P	rs60930717	—	—	—	—	5.1	1.000*	-0.948*	-2.74*	De novo	Choi et al. (2004)
FC930	Tail	c.1319C>T	p.P440L	rs58777882	—	—	—	—	5.02	0.981*	0.694	-1.69*	De novo	Benedetti et al. (2010)
FC264	Tail	c.1327T>A	p.Y443N	rs774761874	—	—	—	0.00087	5.91	0.997*	-0.985*	-1.64*	De novo	This study
FC497	Tail	c.1401G>C	p.K467N	—	—	—	—	—	3.89	0.991*	-0.995*	-1.74*	De novo	This study

Abbreviations: CMT1F, CMT type 1F; CMT2E, CMT type 2E; CMT2DIG, autosomal dominant intermediate CMT type G.

^aReference DNA sequence of NEFL NM_006158.4.

^bVariant allele frequencies in the 1000 Genomes database (Jun 2015, <http://www.1000genomes.org/>).

^cVariant allele frequencies in the Exome Variant Server database (Dec 2014, <http://evs.gs.washington.edu/EVS/>).

^dVariant allele frequencies in the ExAC browser database (Jan 2015, <http://exac.broadinstitute.org/>).

^eVariant allele frequencies in the Korean Reference Genome Database (<http://codan.nih.go.kr/coda/KRGDB/>).

^fGenomic evolutionary rate profiling scores.

^gpolyPhen-2 (PP2) score ~1, MUpro score <0, and Fathmm score ≤-1.5 indicate a prediction of pathogenicity (pathogenic prediction).

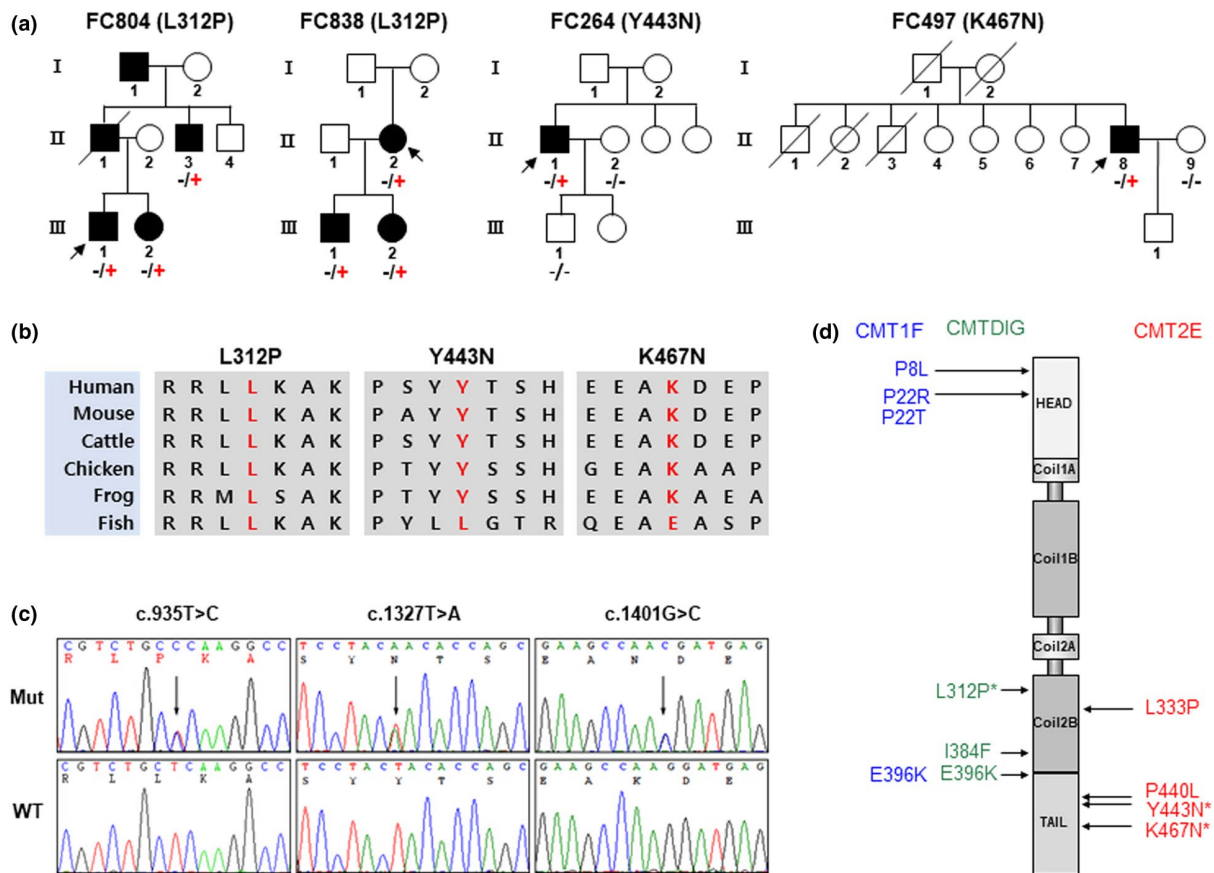


FIGURE 1 Families with novel *NEFL* mutations. (a) The pedigrees and genotypes of four CMT families with novel *NEFL* mutations. (□, ○: unaffected members; ■, ●: affected members). (b) Conservation analysis of amino acid sequences at the mutation sites. The mutation sites and surrounding amino acid sequences are well conserved among different vertebrate species (*H. sapiens* NP_006149.2, *M. musculus* NP_035040.1, *B. taurus* NP_776546.1, *G. gallus* XP_417679.1, *X. tropicalis* XP_002932628.2 and *D. rerio* NP_001034927.1). (c) Sequencing chromatograms of the novel *NEFL* mutations. Vertical arrows indicate the mutation sites (Mut: mutant allele, WT: wild-type allele). (d) Localization of mutations in the *NEFL* protein that cause CMT1F, CMT2E, or CMTDIG. Mutations found in this study are underlined

We identified 10 mutations in the *NEFL* gene, three of which (p.L312P, p.Y443N, and p.K467N) were previously unreported (Table 1, Figure 1). All the novel mutation sites are highly conserved in different vertebrate species (Figure 1b) and were confirmed by Sanger sequencing (Figure 1c). None of the three mutations was reported in the 1000 Genomes project database, Exome Variant Server, or ExAC databases, and several in silico tools (PolyPhen-2: 0.991–0.999; MUpro: –1.000 to –0.985; Fathmm: –2.65 to –1.64) predicted that all three mutations would affect protein function.

The p.P8L, p.P22R, p.P22T, and p.E396K mutations were identified in patients with demyelinating CMT1F, and the p.L312P, p.I384F, and p.E396K mutations were identified in patients with intermediate CMTDIG (Table 1, Figure 1d). Notably, the p.E396K mutation was found in both CMT1F and CMTDIG patients. The p.L333P, p.P440L, p.Y443N, and p.K467N mutations were found in the axonal CMT2E patients. Eight de novo cases (FC549

in CMT1F; FC441, FC838, and FC984 in CMTDIG; and FC21, FC264, FC497, and FC930 in CMT2E) were identified at a rate of 0.47 based on a trio-family analysis (Table 1). This de novo frequency is similar to the rate of 0.40 reported by Horga et al. (2017).

The 3D structure of the *NEFL* protein is predicted to be a continuous coiled coil structure (Figure 2a). When the p.L312 in the coil2B domain is replaced by proline (p.L312P), it is predicted to form two additional hydrogen bonds with T316 and K313 residues (Figure 2b). The p.Y443 and p.K467 residues are located in the tail domain. The aromatic ring of p.Y443 is predicted to form hydrogen bonds with p.S416 and p.P440 residues. However, when the p.Y443 is replaced by asparagine (p.Y443N), a considerable conformational change is predicted, with the abolition of the two hydrogen bonds with S416 and P440 and the formation of new hydrogen bonds with p.S441, p.T444, and p.E449 residues (Figure 2c). The p.K467 is predicted to form several hydrogen bonds with p.E371, p.D374, and

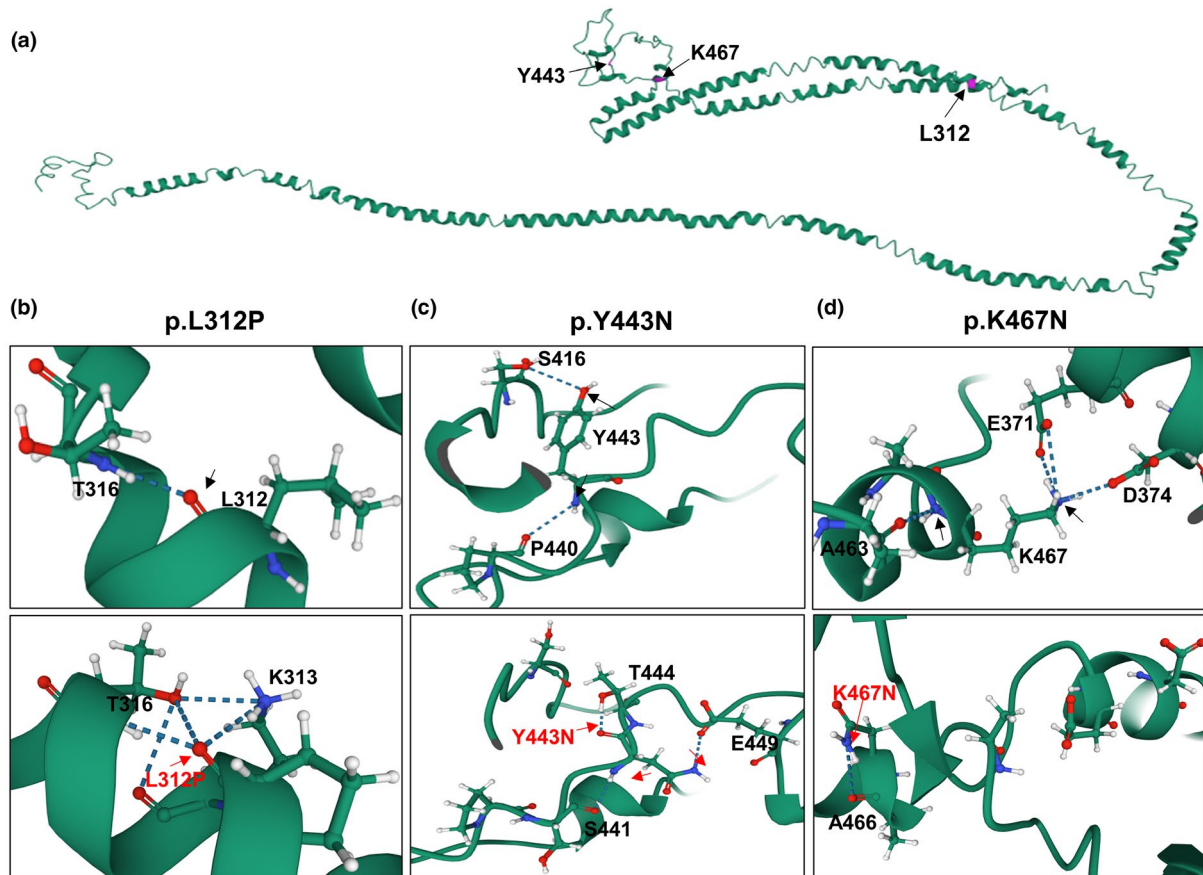


FIGURE 2 Prediction of 3D structural changes in the *NEFL* protein caused by the novel mutations. The 3D structures were predicted using I-TASSER Protein Structure & Function Predictions (<https://zhanglab.cmb.med.umich.edu/I-TASSER>) and visualized using the 3D View feature in Protein Data Bank (<http://www.rcsb.org>). (a) Predicted whole *NEFL* 3D structure. The three novel mutation sites are in red. (b–d) Prediction of the conformational changes caused by p.L312P (b), p.Y443N (c), and K467N (d). Upper and bottom panels indicate wild types and mutant types, respectively (----: hydrogen bond)

p.A463 residues. When the p.K467 is replaced by asparagine (p. K467N), the hydrogen bonds are predicted to brake, and it is newly formed with deformation of helical structure (Figure 2d).

3.2 | Clinical manifestations

The clinical features of 37 Korean *NEFL* patients (20 males and 17 females) from 17 families are shown in Table 2. The frequency was 1.49% of all 1,143 Korean CMT families tested and 2.13% of the 799 families without *PMP22* duplication (Table S1). Five families had CMT1F, eight had CMTDIG, and four had CMT2E. In all Korean CMT families, the frequencies of CMT1F, CMTDIG, and CMT2E harboring *NEFL* mutations were 0.44%, 0.70%, and 0.35%, respectively.

In all patients, muscle weakness and atrophy predominated in the distal parts of the lower extremities, and the proximal portions of the extremities were relatively preserved. Symptoms were noted to a lesser extent distally in

the upper limbs, and clinically obscured nerve hypertrophy was absent. The mean age at onset was 10.2 ± 7.3 years in CMT1F, 12.7 ± 7.9 years in CMTDIG, and 24.3 ± 9.4 years in CMT2E patients (Table 2). The onset age was thus significantly earlier in CMT1F and CMTDIG than in CMT2E ($p < 0.05$). However, disease-related disability according to CMTNS v2 and the FDS did not differ among the *NEFL* subgroups. Length-dependent sensory loss was observed in all patients, and vibration was reduced to a greater extent than pain. Knee and ankle jerks were hyporeflexive or areflexive.

Although most *NEFL*-related patients showed the classical CMT phenotypes harboring peripheral neuropathy, they also revealed additional features, including delayed walking, ataxia, dysphagia, dysarthria, dementia, ptosis, waddling gait, tremor, hearing loss, and abnormal visual evoked potential. Five patients from four families with dominant mutations (P8L, P22R, or E396K) had early onset with delayed motor milestones at or before age 3 years. Gait ataxia was the most common symptom in *NEFL*-related CMT patients: CMT1F (78%), CMTDIG

TABLE 2 Clinical features in 37 CMT patients with NEFL mutations

Patient	Amino acid change	Sex	Age at exam (years)	Age at onset (years)	FDS	CMTNS v2	Distal weakness of arm ^a	Distal weakness of leg ^a	Muscle atrophy	Sensory loss ^b	Knee/ankle jerks ^c	Pes cavus	Other findings
CMT1F													
FC7-1	p.E396K	M	43	8	6	24	++	+++	Moderate	P<V	A/A	Yes	Ataxia, scoliosis, hearing loss
FC7-2	p.E396K	F	5	2	3	ND	+	++	Mild	V	D/D	Yes	Delayed walking, ataxia
FC99-1	p.P22R	M	20	3	4	24	++	+++	Moderate	P<V	A/A	Yes	Delayed walking, ataxia, tremor, abnormal VEP
FC99-2	p.P22R	F	45	13	7	27	++	+++	Severe	P<V	A/A	Yes	Ataxia, scoliosis, hearing loss, tremor
FC99-5	p.P22R	F	55	15	7	32	++	+++	Severe	P<V	A/A	Yes	Hearing loss, dysphagia, tremor
FC99-9	p.P22R	M	44	8	7	28	++	+++	Severe	P<V	A/A	Yes	Dementia, tremor, hearing loss, dysphagia
FC361-1	p.P22T	F	24	23	3	19	+	++	Moderate	P<V	D/D	Yes	Ataxia
FC467-1	p.E396K	M	41	17	3	16	+	++	Moderate	P<V	D/D	Yes	Ataxia
FC549-1	p.P8L	M	15	3	4	23	+	+++	Moderate	V	D/A	Yes	Delayed walking, ataxia, tremor
CMT1G													
FC154-1	p.E396K	M	45	2	7	29	++	+++	Moderate	V	D/A	Yes	Delayed walking, ataxia, waddling gait, scoliosis, hearing loss
FC154-3	p.E396K	M	16	2	4	24	+	+++	Moderate	V	D/A	Yes	Delayed walking, ataxia, waddling gait, scoliosis
FC154-6	p.E396K	M	56	5	5	ND	++	+++	Severe	P<V	A/A	Yes	Ataxia, hearing loss, waddling gait
FC221-1	p.I384F	M	42	9	3	19	+	++	Mild	P<V	D/D	Yes	—
FC221-2	p.I384F	F	36	11	2	16	+	+	Mild	P<V	A/A	Yes	Ataxia
FC221-3	p.I384F	M	19	8	2	20	+	++	Mild	P=V	D/D	Yes	Ataxia
FC221-6	p.I384F	F	46	18	2	12	+	++	Moderate	V	D/D	Yes	Ataxia
FC221-7	p.I384F	F	29	8	3	23	+	++	Mild	V	D/A	Yes	Ataxia
FC221-9	p.I384F	F	40	12	2	14	+	++	Mild	P=V	A/A	Yes	—
FC221-11	p.I384F	F	23	12	2	17	+	++	Mild	P<V	A/A	Yes	—
FC221-15	p.I384F	F	67	35	3	ND	++	+++	Moderate	P<V	A/A	Yes	Ataxia
FC330-1	p.E396K	F	28	11	6	25	++	+++	Severe	P<V	A/A	Yes	Hearing loss, ataxia
FC330-2	p.E396K	F	57	15	7	29	++	+++	Severe	P<V	A/A	Yes	Dementia, hearing loss, tremor

(Continues)

TABLE 2 (Continued)

Patient	Amino acid change	Sex	Age at exam (years)	Age at onset (years)	FDS	CMTNS v2	Distal weakness of arm ^a	Distal weakness of leg ^a	Muscle atrophy	Sensory loss ^b	Knee/ankle jerks ^c	Pes cavus	Other findings
FC330-3	p.E396K	M	31	11	4	24	++	+++	Moderate	P<V	A/A	Yes	Hearing loss, ataxia, tremor
FC441-1	p.E396K	F	14	6	1	7	—	+	No	P=V	N/N	Yes	Hearing loss, ataxia, tremor
FC804-1	p.L312P	M	22	8	2	10	+	++	Mild	V	A/A	Yes	Ataxia
FC804-4	p.L312P	M	47	22	3	15	++	++	Moderate	P<V	A/A	Yes	Ataxia, tremor
FC838-1	p.L312P	F	38	17	2	11	+	++	Moderate	P<V	A/A	Yes	Ataxia, scoliosis
FC838-4	p.L312P	M	6	5	1	5	+	+	Mild	V	D/D	Yes	—
FC984-1	p.E396K	F	46	5	3	16	++	++	Moderate	P<V	D/A	Yes	Ataxia
FC1037-1	p.I384F	M	52	15	4	25	++	+++	Severe	P<V	A/A	Yes	Tremor, hearing loss, ataxia
FC1037-2	p.I384F	F	22	15	1	7	+	+	Mild	V	D/D	Yes	Scoliosis, tremor
FC1037-4	p.I384F	M	59	21	8	34	+++	+++	Severe	P<V	A/A	Yes	Dementia, bed-ridden state, tremor, hearing loss
FC1037-5	p.I384F	M	55	17	4	24	+++	+++	Severe	P<V	A/A	Yes	Ataxia, scoliosis
CMT2E													
FC21-1	p.L333P	M	51	13	7	29	++	+++	Severe	P<V	A/A	Yes	Ptosis, ataxia, hearing loss, tremor, dysarthria, raised CK
FC264-1	p.Y443N	M	37	28	2	9	—	+	Mild	V	N/D	Yes	—
FC497-1	p.K467N	M	46	21	4	24	++	+++	Severe	V	D/A	Yes	Ptosis, dysphagia, dysarthria, tremor, ataxia, hearing loss
FC930-3	p.P440L	F	37	35	0	3	—	+	No	No	D/D	Yes	—

Abbreviations: CK, creatine kinase; CMT1F, CMT type 1F; CMT2E, CMT type 2E; CMTD1G, autosomal dominant intermediate CMT type G; CMTNS v2, CMT neuropathy score version 2; FDS, functional disability scale; VEP, visual evoked potential.

^aMuscle weakness in upper limbs: + = intrinsic hand weakness 4/5 on MRC scale; ++ = intrinsic hand weakness <4/5 on MRC scale; +++ = proximal weakness; — = no symptoms.

^bMuscle weakness in lower limbs: + = ankle dorsiflexion 4/5 on medical research council (MRC) scale; ++ = ankle dorsiflexion <4/5 on MRC scale; +++ = proximal weakness.

^cSensory loss: P = pain sense; V = vibration sense.

^dDeep tendon reflexes: D = diminished; A = absent; N = normal reflex.

(79%), and CMT2E (50%). Patients were tested genetically for spinocerebellar ataxia, but we did not find any relevant mutations. Two patients carrying the L333P and K467N mutations showed dysarthria. Two patients with E396K had an element of proximal weakness in the lower limbs and a waddling gait, which was consistent with previously reported cases (Horga et al., 2017). Early onset dementia was found in patients with CMT1F and CMTDIG. Interestingly, ptosis was frequently (50%) and predominantly observed in CMT2E patients.

The p.E396K mutation was identified in two CMT1F and four CMTDIG families. The heterogeneity of phenotypes caused by the p.E396K mutation was found according to the variation in the age at onset, which ranges from 2 years to second decade. This heterogeneity among patients was also found in FDS (raged from 1 to 7) and CMTNS v2 (raged from 7 to 29). Moreover, the patients with p.E396K exhibited ranged from absence to severe muscle atrophy.

3.3 | Electrophysiological findings

Neurophysiological studies were done in 34 affected individuals (19 males and 15 females) (Table 3). In the CMT1F patients, the amplitudes of evoked peroneal motor responses were often markedly decreased, and in six of eight patients (75%), amplitudes could not be recorded. However, in the CMT2E patients, peroneal amplitudes were not obtained for only one of four patients (25%). Interestingly, the CMTDIG group was situated in the middle between the CMT1F and CMT2E groups (36%). Among CMT1F patients, the mean MNCVs of the median nerve were 16.1 ± 10.5 m/s (range 0–28.5 m/s), and all of them had median MNCVs below 38 m/s. In CMT2E patients, the mean MNCVs of the median nerve were 47.7 ± 8.1 m/s (range 40.6–56.2 m/s). The median MNCVs of CMTDIG patients were 39.7 ± 4.4 m/s (range 32.9–49.0 m/s). No SNAPs of the median nerve were found in 63% of CMT1F patients, 32% of CMTDIG patients, and 25% of CMT2E patients. Also, sural SNAPs were not evoked in any of the CMT1F patients nor were they found in 36% of CMTDIG patients and 25% of CMT2E patients.

3.4 | Fatty infiltration in the lower limb muscles

The results of MRI analyses are summarized in Tables S2 and S3. Intramuscular fat infiltration was generally more severe in the distal calf muscles than in the proximal calf muscles and thigh muscles, demonstrated as a higher

Goutallier grade in an analysis of T1-weighted MRIs, which is consistent with the hypothesis of length-dependent neuropathic degeneration (Figure 3a–f). Comparing patients with similar disease duration but different clinical features, we found notable differences in the degree and pattern of muscular fat infiltration depending on the subtype of *NEFL* mutation. In the MRI of a CMT1F patient (FC99-1) taken at age 22 (disease duration 19 years), moderate to severe fat infiltration is seen in the anterior compartment muscles of the mid- and distal thigh. In contrast, the thigh MRIs of a CMTDIG patient (FC838-1, age 37; disease duration 20 years) and a CMT2E patient (FC264-1, age 47; disease duration 19 years) showed mild and minimal fat infiltration, respectively. In the calf muscles, the CMT1F patient (FC99-1) showed severe fat infiltration in all the muscle compartments (anterolateral, superficial, and deep posterior) at the proximal and distal levels. The CMTDIG patient (FC838-1) showed the most severe fat infiltration in the superficial posterior compartment muscles at proximal and distal level, and the CMT2E patient (FC264-1) had the most pronounced fat infiltration in the anterolateral compartment at the distal calf.

Mean cross-sectional areas of sciatic nerves were 30.06 ± 7.00 mm² at level 1, 31.55 ± 9.41 mm² at level 2, and 26.11 ± 5.59 mm² at level 3 (Table S4). Compared with previously reported cross-sectional areas of sciatic nerves in CMT1A patients and healthy controls measured at same levels, measured cross-sectional areas of *NEFL*-related CMT patients in our study do not show evidence of nerve hypertrophy (Kim et al., 2019).

We observed a sequential pattern of fatty infiltration of muscles within families with different disease durations and severities (Figures S1 and S2). In the CMT1F family (FC99), diffuse fatty infiltration of all compartments of the calf muscles was observed in the early disease stage (Figure S1g, j). At the thigh level, there was selective fatty infiltration in the vastus lateralis muscles and to a lesser degree in the semitendinosus muscles. However, the adductor muscle groups were relatively spared (Figure S1a, d). In the CMTDIG family (FC330), selective and severe fatty infiltration of the soleus muscles occurred in the early disease stage (Figure S2g–l). At the thigh level, the semitendinosus muscles were initially involved, but the vastus lateralis and adductor muscles were relatively spared (Figure S2a–f).

4 | DISCUSSION

In this study, we identified 10 causative *NEFL* missense mutations in 37 Korean CMT patients, and we found phenotypic diversity in clinical, electrophysiological, and neuroimaging features. Three of the 10 mutations (p.L312P,

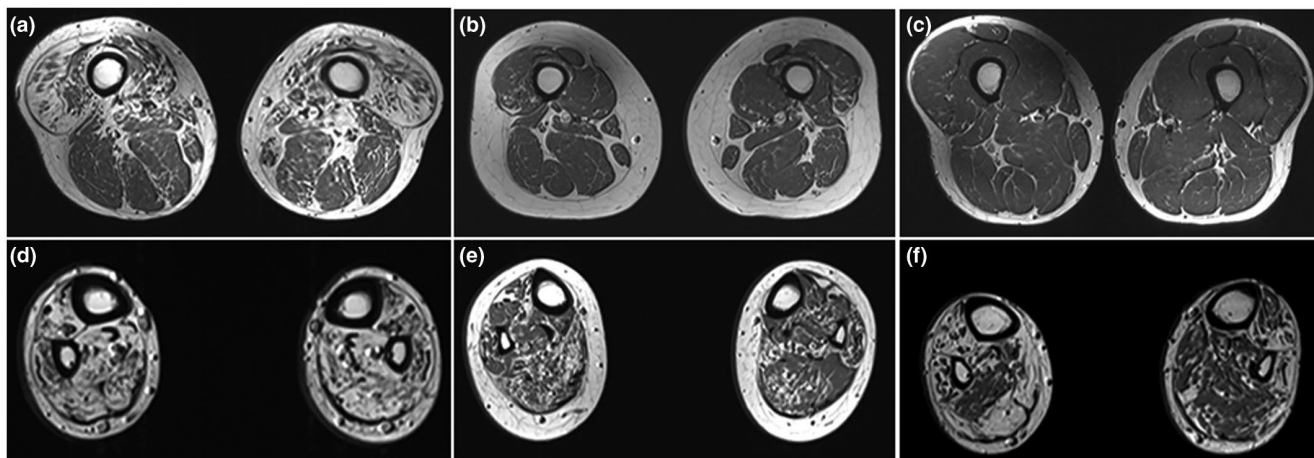


FIGURE 3 Axial T1-weighted MRIs of the thigh (a–c) and calf (d–f) in *NEFL* patients with similar disease durations. CMT1F (a, d) in FC99-1 [male/22 years, disease duration (DD) = 19 years], CMTDIG (b, e) in FC838-1 (female/37 years, DD = 20 years), and CMT2E (c, f) in FC264-1 (II-1, male/47 years, DD = 19 years). (a) Distal thigh of the CMT1F patient shows severe fat infiltration in the anterior compartment muscles. (b) Distal thigh of the CMTDIG patient shows only mild fat infiltration in the vastus lateralis muscle. (c) Distal thigh of the CMT2E patient shows minimal fat infiltration. (d) Distal calf of the CMT1F patient shows severe fat infiltration in all the muscle compartments (anterolateral, superficial, and deep posterior compartments). (e) In the distal calf of the CMTDIG patient, the superficial posterior compartment muscle had severe fat infiltration. (f) In the distal calf of the CMT2E patient, the anterior and lateral compartment muscles were most severely affected

p.Y443N, p.K467N) were determined to be novel, and we report six new patients harboring those novel mutations (Table 2). Three novel mutations were determined to be “likely pathogenic” according to ACMG guideline. All of these mutations cause amino acid substitutions with different properties and involve regions highly conserved between species. The loci of CMT1F were the head and coil2B domains, and those of CMT2E were the coil2B and tail. The mutation sites of CMTDIG were only in the coil2B domain (Table 2, Figure 2).

Data on the frequency of *NEFL* gene mutations are very limited, though the relevance of the *NEFL* mutation in CMT has rarely been reported to be below 1% (Table S1). *NEFL* mutation frequency was detected in the range of 0.9–2.3% in Japanese (Abe et al., 2009; Yoshimura et al., 2018) and Chinese (Hsu et al., 2019) cohorts and in this study (Table S1) (Yoshimura et al., 2018). Therefore, the mutation frequency observed in East Asian countries is higher than that reported in other countries (DiVincenzo et al., 2014; Fridman et al., 2015; Gess et al., 2013; Hsu et al., 2019; Manganeli et al., 2014; Murphy et al., 2012; Østern et al., 2013; Rudnik-Schöneborn et al., 2016; Saporta et al., 2011; Sivera et al., 2013; Yoshimura et al., 2018) Although additional evidence from other population studies is needed, ethnic differences might be involved.

The mode of transmission is usually autosomal dominance, although 36% of the kindred in our study were classified as de novo cases. Disease onset varied between the first and fourth decades of life, and 46% of patients had first decade onset presentation. Five patients (13.5%)

had early onset with delayed motor milestones at or before age 3 years. Distal lower extremity–predominant muscle weakness and atrophy and length-dependent sensory loss exclusively in the vibration modality were commonly observed. The phenotypic descriptions of 17 families concur, and the severity of these phenotypes was consistent among siblings in individual families. It has been known that ambulation is generally preserved throughout life, but in this study, six patients (16%) were wheelchair bound, and one patient (3%) was bedridden.

Our electrophysiological findings show differences among the three subgroups (Table 3). In the CMT1F group, MNCVs were markedly reduced, to the extent that peroneal CMAPs were not recordable in 75% of patients. However, in the CMT2E group, peroneal nerve conduction was recordable in 75% of patients. In all subtypes, sensory electrophysiological data indicate more prominent impairment than those for motor function. Neurophysiologically, *NEFL*-related CMT was classified as demyelinating, axonal, and intermediate neuropathy in 24.3%, 10.8%, and 64.9% of cases, respectively.

CMTDIG with *NEFL* mutation was first described by Berciano et al. (2015), and we found eight dominant intermediate CMT families. Moreover, we identified the novel p.L312P mutation that causes CMTDIG. In FC804 and FC838 with p.L312P, nerve conduction studies showed a uniform slowing of MNCVs for the median nerve that ranged from 36.5 to 46.4 m/s, which is in the intermediate range. The incidence of CMTDIG was twice as high as that reported by Horga et al. (2017) Therefore, it is likely that

CMTDIG is more common among Asian patients than in Western countries, we could not exclude that the difference is due to a chance effect by the small sample size.

The p.E396K mutation was identified in six families, two CMT1F and four CMTDIG families, which indicates remarkable clinical heterogeneity. In the two CMT1F families (FC7 and FC467), the range of median MNCVs was from 19.2 to 23.1 m/s. Although the patients had the same genetic mutation, clinical and electrophysiological examinations showed typical demyelinating neuropathy, CMT1 type. Previously, p.E396K was reported to cause only CMT2E or CMTDIG. Therefore, this is the first study to show the CMT1F phenotype with that mutation (Abe et al., 2009; Berciano et al., 2015; Fabrizi et al., 2007; Lin et al., 2011). The high occurrence of the c.1186G>A point mutation on the E396K mutation could be because it is located within a CpG dinucleotide, which has a high chance of spontaneous transition. The p.E396K mutation changes the guanine at the 1186 codon of the third exon to adenine, which changes a negatively charged glutamic acid to a positively charged lysine. That mutation is located between 393 and 398, a well-preserved motive protein that sends signals to the terminal region of the rod area, and the mutation is thought to cause a significant change in the structure of that region, producing neuropathy (Perez-Olle et al., 2002). Therefore, this particular *NEFL* mutation can produce different clinical features.

It is interesting that some patients with *NEFL* mutations have shown symptoms of central nervous system (CNS) involvement (Adebola et al., 2015; Berciano et al., 2015, 2016; Hashiguchi et al., 2014; Miltenberger-Miltenyi et al., 2007; Yum et al., 2009). We also found evidence of CNS involvement in all three subtypes of patients with *NEFL* mutations (Berciano et al., 2016; Mersyanova et al., 2000). Both those results strongly suggest that *NEFL* mutation has the potential to cause CNS symptoms. The expression of the neurofilament light chain is restricted to specific types of neuronal cells in the CNS and peripheral nervous system (PNS). An experimental mouse model of *NEFL*^{N98S/+} exhibited multiple inclusions in the cell bodies and proximal axons of the spinal cord, cerebellum, pons, and cerebral cortex (Adebola et al., 2015). Those findings provide evidence for the simultaneous involvement of the PNS and CNS. In this study, we found that *NEFL* mutations could be characterized by subclinical CNS involvement, including delayed walking, ataxia, dysphagia, dysarthria, dementia, ptosis, waddling gait, tremor, hearing loss, and abnormal visual evoked potential, which also suggests the simultaneous involvement of the PNS and CNS. Although no structural lesions were identified in the brain MRIs, further evaluations such as diffusion

tensor images or transmagnetic stimulations would be needed to find evidence of functional CNS involvement. According to a previously reported diffusion tensor imaging paper, changes in brain imaging were found in patients with *NEFL* mutations (Lee et al., 2017).

Our MRI analyses reveal varying degrees of intramuscular fat infiltration in the lower extremity muscles of *NEFL* patients. MRIs have been useful for finding patterns of amyotrophy in CMT. Our MRI results for fat infiltration indicate that the distal parts of the extremities were more affected, which is consistent with the hypothesis of length-dependent neuropathic degeneration. It has been reported that CMTDIG patients with the *NEFL* E396K mutation had marked atrophy in their distal portions, predominating in posterior muscles innervated by the tibial nerve (T-type) (Berciano et al., 2015). The most severe fatty hyperintense signal changes in our CMTDIG patients were also of the T-type, which was different from the findings in our CMT1F and CMT2E patient groups. As far as we know, no previous reports have described lower extremity MRI findings from CMT1F and CMT2E patients. In CMT1F patients, all four muscle group compartments were involved evenly (whole muscle involvement in the calf through the peroneal and tibial nerves; W-type). In contrast, the anterior and lateral muscle groups were most severely affected in CMT2E patients (P-type). When we compared patients with similar disease durations but different clinical features, we found that the severity of atrophy and fatty infiltration in the muscles increased according to the subtype of CMT in the order CMT1F, CMT2E, and CMTDIG. Sequential progress patterns of muscle involvement within the same family were observed in CMT1F and CMTDIG. At the thigh level in the CMT1F family (FC99), there was a tendency for the anterior compartment muscles (innervated by the femoral nerve; F-type) to be involved and, to a lesser degree, the posterior compartment muscles (innervated by the sciatic nerve; S-type), with the adductor muscle groups (innervated by the obturator nerve; O-type) relatively spared. That result suggests that the lower limb amyotrophy in CMT1F is W-type in the calf and F-type >S-type >O-type in the thigh. In the CMTDIG family (FC330), we observed selective and severe fatty infiltration of soleus muscles (T-type) at the early disease stage. At the thigh level, selective severe involvement of the vastus lateralis muscles (F-type) was observed, and a lesser degree of involvement was observed in the semitendinosus muscles (S-type), with the adductor muscle groups (O-type) relatively spared. As a result, the current pattern of lower limb amyotrophy for CMTDIG is T-type >P-type >F-type >S-type >O-type. Those findings will be helpful in investigating the pathomechanism of developing disease caused by different site mutations in the same *NEFL* gene.

In this study, we have shown the phenotypic heterogeneities of Korean CMT patients with *NEFL* mutations. The identified variant CNS clinical features could be useful in the differential diagnosis of *NEFL*-related CMT against other forms of CMT. The clinical, genetic, and neuroimaging results of this study will also be helpful in the evaluation of novel *NEFL* variants.

ETHICS APPROVAL AND CONSENT TO PARTICIPATE

This study was approved by the Institutional Review Boards of Sungkyunkwan University, Samsung Medical Center (2014-08-057-002), and Kongju National University (KNU-IRB-2018-62). Written informed consent was obtained from all participants.

ACKNOWLEDGMENTS

We would like to thank all the affected individuals and their family members who participated in this study. This work was supported by grants from the National Research Foundation (2019R1A2C1087547, 2020M3H4A1A03084600, and 2021R1A4A2001389) and the Korean Health Technology R&D Project, Ministry of Health and Welfare (HI14C3484 and HI20C0039), Republic of Korea.

CONFLICT OF INTEREST

The authors have declared no conflict of interest.

AUTHOR CONTRIBUTIONS

BOC and KWC planned and supervised this study. HJK, SHN, HMK, and SOL performed the molecular genetic work. HSK and JHP performed the clinical and neuroimaging work. HJK, KSL, JEL, AJL, and KWC interpreted genetic data and conducted the statistical analyses. BOC collected the participant samples and information. HJK, BOC, and KWC wrote the manuscript. All the co-authors read and approved the final version of the manuscript.

DATA AVAILABILITY STATEMENT

All raw genetic and clinical data generated or analyzed during this study are available upon request to the corresponding author.

ORCID

Hye Jin Kim  <https://orcid.org/0000-0002-7636-3639>

Ki Wha Chung  <https://orcid.org/0000-0003-0363-8432>

Byung-Ok Choi  <https://orcid.org/0000-0001-5459-1772>

REFERENCES

Abe, A., Numakura, C., Saito, K., Koide, H., Oka, N., Honma, A., Kishikawa, Y., & Hayasaka, K. (2009). Neurofilament light

chain polypeptide gene mutations in Charcot–Marie–Tooth disease: nonsense mutation probably causes a recessive phenotype. *Journal of Human Genetics*, 54(2), 94–97. <https://doi.org/10.1038/jhg.2008.13>

- Adebola, A. A., Di Castri, T., He, C.-Z., Salvatierra, L. A., Zhao, J., Brown, K., Lin, C.-S., Worman, H. J., & Liem, R. K. H. (2015). Neurofilament light polypeptide gene N98S mutation in mice leads to neurofilament network abnormalities and a Charcot–Marie–Tooth Type 2E phenotype. *Human Molecular Genetics*, 24(8), 2163–2174. <https://doi.org/10.1093/hmg/ddu736>
- Benedetti, S., Previtali, S. C., Coviello, S., Scarlato, M., Cerri, F., Di Pierri, E., Piantoni, L., Spiga, I., Fazio, R., Riva, N., Natali Sora, M. G., Dacci, P., Malaguti, M. C., Munerati, E., Grimaldi, L. M. E., Marrosu, M. G., De Pellegrin, M., Ferrari, M., Comi, G., ... Bolino, A. (2010). Analyzing histopathological features of rare Charcot–Marie–tooth neuropathies to unravel their pathogenesis. *Archives of Neurology*, 67(12), 1498–1505. <https://doi.org/10.1001/archneurol.2010.303>
- Berciano, J., García, A., Peeters, K., Gallardo, E., De Vriendt, E., Pelayo-Negro, A. L., Infante, J., & Jordanova, A. (2015). *NEFL* E396K mutation is associated with a novel dominant intermediate Charcot–Marie–Tooth disease phenotype. *Journal of Neurology*, 262(5), 1289–1300. <https://doi.org/10.1007/s00415-015-7709-4>
- Berciano, J., Peeters, K., García, A., López-Alburquerque, T., Gallardo, E., Hernández-Fabián, A., Pelayo-Negro, A. L., De Vriendt, E., Infante, J., & Jordanova, A. (2016). *NEFL* N98S mutation: Another cause of dominant intermediate Charcot–Marie–Tooth disease with heterogeneous early-onset phenotype. *Journal of Neurology*, 263(2), 361–369. <https://doi.org/10.1007/s00415-015-7985-z>
- Birouk, N., LeGuern, E., Maisonnobe, T., Rouger, H., Gouider, R., Tardieu, S., Gugenheim, M., Routon, M. C., Leger, J. M., Agid, Y., Brice, A., & Bouche, P. (1998). X-linked Charcot–Marie–Tooth disease with connexin 32 mutations: Clinical and electrophysiologic study. *Neurology*, 50(4), 1074–1082. <https://doi.org/10.1212/WNL.50.4.1074>
- Choi, B.-O., Koo, S. K., Park, M.-H., Rhee, H., Yang, S.-J., Choi, K.-G., Jung, S.-C., Kim, H. S., Hyun, Y. S., Nakhro, K., Lee, H. J., Woo, H.-M., & Chung, K. W. (2012). Exome sequencing is an efficient tool for genetic screening of Charcot–Marie–Tooth Disease. *Human Mutation*, 33(11), 1610–1615. <https://doi.org/10.1002/humu.22143>
- Choi, B.-O., Lee, M. S., Shin, S. H., Hwang, J. H., Choi, K.-G., Kim, W.-K., Sunwoo, I. N., Kim, N. K., & Chung, K. W. (2004). Mutational analysis of PMP22, MPZ, GJB1, EGR2 and *NEFL* in Korean Charcot–Marie–Tooth neuropathy patients. *Human Mutation*, 24(2), 185–186. <https://doi.org/10.1002/humu.9261>
- DiVincenzo, C., Elzinga, C. D., Medeiros, A. C., Karbassi, I., Jones, J. R., Evans, M. C., Braastad, C. D., Bishop, C. M., Jaremko, M., Wang, Z., Liaquat, K., Hoffman, C. A., York, M. D., Batish, S. D., Lupski, J. R., & Higgins, J. J. (2014). The allelic spectrum of Charcot–Marie–Tooth disease in over 17,000 individuals with neuropathy. *Molecular Genetics & Genomic Medicine*, 2(6), 522–529. <https://doi.org/10.1002/mgg3.106>
- Fabrizi, G. M., Cavallaro, T., Angiari, C., Cabrini, I., Taioli, F., Malerba, G., Bertolasi, L., & Rizzuto, N. (2007). Charcot–Marie–Tooth disease type 2E, a disorder of the cytoskeleton. *Brain*, 130, 394–403.

- Fridman, V., Bundy, B., Reilly, M. M., Pareyson, D., Bacon, C., Burns, J., Day, J., Feely, S., Finkel, R. S., Grider, T., Kirk, C. A., Herrmann, D. N., Laurá, M., Li, J., Lloyd, T., Sumner, C. J., Muntoni, F., Piscoquito, G., Ramchandren, S., ... Shy, M. E. (2015). CMT subtypes and disease burden in patients enrolled in the Inherited Neuropathies Consortium natural history study: A cross-sectional analysis. *Journal of Neurology, Neurosurgery & Psychiatry*, *86*(8), 873–878. <https://doi.org/10.1136/jnnp-2014-308826>
- Gess, B., Schirmacher, A., Boentert, M., & Young, P. (2013). Charcot-Marie-Tooth disease: Frequency of genetic subtypes in a German neuromuscular center population. *Neuromuscular Disorders*, *23*, 647–651. <https://doi.org/10.1016/j.nmd.2013.05.005>
- Goutallier, D., Postel, J. M., Bernageau, J., Lavau, L., & Voisin, M. C. (1994). Fatty muscle degeneration in cuff ruptures. Pre- and postoperative evaluation by CT scan. *Clinical Orthopaedics and Related Research*, *304*, 78–83. <https://doi.org/10.1097/00003086-199407000-00014>
- Hashiguchi, A., Higuchi, Y., Nomura, M., Nakamura, T., Arata, H., Yuan, J., Yoshimura, A., Okamoto, Y., Matsuura, E., & Takashima, H. (2014). Neurofilament light mutation causes hereditary motor and sensory neuropathy with pyramidal signs. *Journal of the Peripheral Nervous System*, *19*(4), 311–316. <https://doi.org/10.1111/jns.12102>
- Horga, A., Laurá, M., Jaunmuktane, Z., Jerath, N. U., Gonzalez, M. A., Polke, J. M., Poh, R., Blake, J. C., Liu, Y. T., Wiethoff, S., & Bettencourt, C. (2017). Genetic and clinical characteristics of *NEFL*-related Charcot-Marie-Tooth disease. *Journal of Neurology, Neurosurgery and Psychiatry*, *88*, 575–585.
- Hsu, Y.-H., Lin, K.-P., Guo, Y.-C., Tsai, Y.-S., Liao, Y.-C., & Lee, Y.-C. (2019). Mutation spectrum of Charcot-Marie-Tooth disease among the Han Chinese in Taiwan. *Annals of Clinical and Translational Neurology*, *6*(6), 1090–1101. <https://doi.org/10.1002/acn3.50797>
- Jordanova, A., De Jonghe, P., Boerkoel, C. F., Takashima, H., De Vriendt, E., Ceuterick, C., Martin, J. J., Butler, I. J., Mancias, P., Pappasozomenos, S. C., & Terespolsky, D. (2003). Mutations in the neurofilament light chain gene (*NEFL*) cause early onset severe Charcot-Marie-Tooth disease. *Brain*, *126*, 590–597. <https://doi.org/10.1093/brain/awg059>
- Kim, H. S., Yoon, Y. C., Choi, B.-O., Jin, W., Cha, J. G., & Kim, J.-H. (2019). Diffusion tensor imaging of the sciatic nerve in Charcot-Marie-Tooth disease type I patients: A prospective case-control study. *European Radiology*, *29*(6), 3241–3252. <https://doi.org/10.1007/s00330-018-5958-1>
- Lee, A. J., Nam, D. E., Choi, Y. J., Nam, S. H., Choi, B. O., & Chung, K. W. (2020). Alanyl-tRNA synthetase 1 (*AARS1*) gene mutation in a family with intermediate Charcot-Marie-Tooth neuropathy. *Genes Genomics*, *42*, 663–672. <https://doi.org/10.1007/s13258-020-00933-9>
- Lee, M., Park, C. H., Chung, H. K., Kim, H. J., Choi, Y., Yoo, J. H., Yoon, Y. C., Hong, Y. B., Chung, K. W., Choi, B. O., & Lee, H. W. (2017). Cerebral white matter abnormalities in patients with Charcot-Marie-Tooth disease. *Annals of Neurology*, *81*, 147–151. <https://doi.org/10.1002/ana.24824>
- Lin, K.-P., Soong, B.-W., Yang, C.-C., Huang, L.-W., Chang, M.-H., Lee, I.-H., Antonellis, A., & Lee, Y.-C. (2011). The mutational spectrum in a cohort of Charcot-Marie-Tooth Disease Type 2 among the Han Chinese in Taiwan. *PLoS One*, *6*(12), e29393. <https://doi.org/10.1371/journal.pone.0029393>
- Manganelli, F., Tozza, S., Pisciotto, C., Bellone, E., Iodice, R., Nolano, M., Geroldi, A., Capponi, S., Mandich, P., & Santoro, L. (2014). Charcot-Marie-Tooth disease: Frequency of genetic subtypes in a Southern Italy population. *Journal of the Peripheral Nervous System*, *19*(4), 292–298. <https://doi.org/10.1111/jns.12092>
- Mersiyanova, I. V., Perepelov, A. V., Polyakov, A. V., Sitnikov, V. F., Dadali, E. L., Oparin, R. B., Petrin, A. N., & Evgrafov, O. V. (2000). A new variant of Charcot-Marie-Tooth disease type 2 is probably the result of a mutation in the neurofilament-light gene. *The American Journal of Human Genetics*, *67*(1), 37–46. <https://doi.org/10.1086/302962>
- Miltenberger-Miltenyi, G., Janecke, A. R., Wanschitz, J. V., Timmerman, V., Windpassinger, C., Auer-Grumbach, M., & Löscher, W. N. (2007). Clinical and electrophysiological features in charcot-marie-tooth disease with mutations in the *NEFL* gene. *Archives of Neurology*, *64*(7), 966–970. <https://doi.org/10.1001/archneur.64.7.966>
- Murphy, S. M., Laura, M., Fawcett, K., Pandraud, A., Liu, Y.-T., Davidson, G. L., Rossor, A. M., Polke, J. M., Castleman, V., Manji, H., Lunn, M. P. T., Bull, K., Ramdharry, G., Davis, M., Blake, J. C., Houlden, H., & Reilly, M. M. (2012). Charcot-Marie-Tooth disease: Frequency of genetic subtypes and guidelines for genetic testing. *Journal of Neurology, Neurosurgery & Psychiatry*, *83*(7), 706–710. <https://doi.org/10.1136/jnnp-2012-302451>
- Østern, R., Fagerheim, T., Hjellnes, H., Nygård, B., Mellgren, S. I., & Nilssen, Ø. (2013). Diagnostic laboratory testing for Charcot Marie Tooth disease (CMT): The spectrum of gene defects in Norwegian patients with CMT and its implications for future genetic test strategies. *BMC Medical Genetics*, *14*, 94. <https://doi.org/10.1186/1471-2350-14-94>
- Paternostro-Sluga, T., Grim-Stieger, M., Posch, M., Schuhfried, O., Vacariu, G., Mittermaier, C., Bittner, C., & Fialka-Moser, V. (2008). Reliability and validity of the Medical Research Council (MRC) scale and a modified scale for testing muscle strength in patients with radial palsy. *Journal of Rehabilitation Medicine*, *40*(8), 665–671. <https://doi.org/10.2340/16501977-0235>
- Perez-Olle, R., Leung, C. L., & Liem, R. K. (2002). Effects of Charcot-Marie-Tooth-linked mutations of the neurofilament light subunit on intermediate filament formation. *Journal of Cell Science*, *115*, 4937–4946. <https://doi.org/10.1242/jcs.00148>
- Previtali, S. C., Zerega, B., Sherman, D. L., Brophy, P. J., Dina, G., King, R. H., Salih, M. M., Feltri, L., Quattrini, A., Ravazzolo, R., & Wrabetz, L. (2003). Myotubularin-related 2 protein phosphatase and neurofilament light chain protein, both mutated in CMT neuropathies, interact in peripheral nerve. *Human Molecular Genetics*, *12*, 1713–1723. <https://doi.org/10.1093/hmg/ddg179>
- Richards, S., Aziz, N., Bale, S., et al. (2015). Standards and guidelines for the interpretation of sequence variants: A joint consensus recommendation of the American College of Medical Genetics and Genomics and the Association for Molecular Pathology. *Genetics in Medicine*, *17*, 405–424.
- Rossor, A. M., Polke, J. M., Houlden, H., & Reilly, M. M. (2013). Clinical implications of genetic advances in Charcot-Marie-Tooth disease. *Nature Reviews. Neurology*, *9*, 562–571. <https://doi.org/10.1038/nrneurol.2013.179>
- Rudnik-Schöneborn, S., Tölle, D., Senderek, J. et al (2016). Diagnostic algorithms in Charcot-Marie-Tooth neuropathies: Experiences

- from a German genetic laboratory on the basis of 1206 index patients. *Clinical Genetics*, 89, 34–43. <https://doi.org/10.1111/cge.12594>
- Sadjadi, R., Reilly, M. M., Shy, M. E., Pareyson, D., Laura, M., Murphy, S., Feely, S. M. E., Grider, T., Bacon, C., Piscoquito, G., Calabrese, D., & Burns, T. M. (2014). Psychometrics evaluation of Charcot-Marie-Tooth Neuropathy Score (CMTNSv2) second version, using Rasch analysis. *Journal of the Peripheral Nervous System*, 19(3), 192–196. <https://doi.org/10.1111/jns.12084>
- Saporta, A. S., Sottile, S. L., Miller, L. J., Feely, S. M., Siskind, C. E., & Shy, M. E. (2011). Charcot-Marie-Tooth disease subtypes and genetic testing strategies. *Annals of Neurology*, 69, 22–33. <https://doi.org/10.1002/ana.22166>
- Shin, J. S., Chung, K. W., Cho, S. Y., Yun, J., Hwang, S. J., Kang, S. H., Cho, E. M., Kim, S.-M., & Choi, B.-O. (2008). NEFL Pro22Arg mutation in Charcot-Marie-Tooth disease type 1. *Journal of Human Genetics*, 53(10), 936–940. <https://doi.org/10.1007/s10038-008-0333-8>
- Sivera, R., Sevilla, T., Vilchez, J. J., Martinez-Rubio, D., Chumillas, M. J., Vazquez, J. F., Muelas, N., Bataller, L., Millan, J. M., Palau, F., & Espinos, C. (2013). Charcot-Marie-Tooth disease: Genetic and clinical spectrum in a Spanish clinical series. *Neurology*, 81(18), 1617–1625. <https://doi.org/10.1212/WNL.0b013e3182a9f56a>
- Yoshihara, T., Yamamoto, M., Hattori, N., Misu, K.-I., Mori, K., Koike, H., & Sobue, G. (2002). Identification of novel sequence variants in the neurofilament-light gene in a Japanese population: Analysis of Charcot-Marie-Tooth disease patients and normal individuals. *Journal of the Peripheral Nervous System*, 7(4), 221–224. <https://doi.org/10.1046/j.1529-8027.2002.02028.x>
- Yoshimura, A., Yuan, J.-H., Hashiguchi, A., Ando, M., Higuchi, Y., Nakamura, T., Okamoto, Y., Nakagawa, M., & Takashima, H. (2019). Genetic profile and onset features of 1005 patients with Charcot-Marie-Tooth disease in Japan. *Journal of Neurology, Neurosurgery & Psychiatry*, 90(2), 195–202. <https://doi.org/10.1136/jnnp-2018-318839>
- Yuan, A., Rao, M. V., & Veeranna, N. R. A. (2012). Neurofilaments at a glance. *Journal of Cell Science*, 125, 3257–3263. <https://doi.org/10.1242/jcs.104729>
- Yum, S. W., Zhang, J., Mo, K., Li, J., & Scherer, S. S. (2009). A novel recessive NEFL mutation causes a severe, early-onset axonal neuropathy. *Annals of Neurology*, 66, 759–770.

SUPPORTING INFORMATION

Additional supporting information may be found in the online version of the article at the publisher's website.

How to cite this article: Kim, H. J., Kim, S. B., Kim, H. S., Kwon, H. M., Park, J. H., Lee, A. J., Lim, S. O., Nam, S. H., Hong, Y. B., Chung, K. W., & Choi, B.-O. (2022). Phenotypic heterogeneity in patients with NEFL-related Charcot-Marie-Tooth disease. *Molecular Genetics & Genomic Medicine*, 10, e1870. <https://doi.org/10.1002/mgg3.1870>